RSC Advances

ROYAL SOCIETY OF CHEMISTRY

www.rsc.org/advances

Catalytic oxidation of 4-chlorophenol with magnetic Fe_3O_4 nanoparticles: mechanisms and particles transformation

Rong Cheng*, Guan-qing Li, Can Cheng, Lei Shi, Xiang Zheng, Zhong Ma*

School of Environment and Natural Resources, Renmin University of China, Beijing 100872, China

Abstract: Magnetite (Fe_3O_4) is usually supposed to be inert and combines with metal catalysts or enzyme to form a composite both of magnetism and catalytic activity. However, it's reported that Fe_3O_4 nanoparticles was of intrinsic peroxidase-like activity. In this study, super paramagnetic Fe_3O_4 nanoparticles with a diameter of about 30 nm were synthesized using self-designed experimental devices under mild conditions. And 4-chlorophenol (4-CP), which is a priority pollutant widely exist in environment but recalcitrant towards chemical and biological degradation, was used as the model compound to test the catalytic activity of synthesized Fe_3O_4 nanoparticles and analysis the mechanisms for 4-CP removal. Besides, surface analysis techniques such as SEM, XRD and Raman spectrum were used to investigate the transformation of nanoparticles and verify the interaction between nanoparticles and 4-CP further. The results revealed that the synthesized Fe_3O_4 nanoparticles showed high catalytic activity even after being used several times, and acidic condition was favourable for dechlorination of 4-CP. However, 4-CP could also be degraded under neutral and alkali conditions. In the process 4-CP was transformed to formic acid, acetic acid and other byproducts. Adsorption test indicated that the

* To whom correspondence should be addressed. Tel: +86-010-62512798; Email: chengrong@ruc.edu.cn; zhongma@vip.sina.com; fax number: +86-010-62512798.

adsorption process didn't play an important role for 4-CP removal, but it did occur between 4-CP and Fe_3O_4. The surface morphology of Fe_3O_4 nanoparticles changed a lot and the reactive sites on the surface increased which resulted in the higher activity of particles after being used. The crystal structure of nanoparticles didn't change, suggesting the role of Fe_3O_4 nanoparticles as catalysts. And Raman spectrum reflected that the adsorption and catalytic oxidation were surface reaction processes. It's proposed that hydroxyl radical produced during reaction was the main cause for degradation of 4-CP. The reaction of H_2O_2 with ferrous to produce hydroxyl radical was the initiate step, and very important for the overall process.

Keywords: Fe_3O_4 nanoparticles; 4-chlorophenol; catalytic activity; mechanisms; iron nanoparticles.

1. Introduction

As important chemical raw materials, chlorophenols have been widely used in pesticide, medicine, dyes and synthetic materials (Zhang et al., 2007). The exposure of chlorophenols poses a serious problem to environment. As a result, chlorophenols are tagged as the hazardous and top priority pollutants by the USEPA (Environmental Protection Agency) due to their toxicity, carcinogenicity, and intractability (Ruzgas et al., 1995; Hwang et al., 2015). In addition, chlorophenols are highly toxic and recalcitrant towards chemical and biological degradation in the environment. Hence the treatment of chlorophenols has been one of the hot topics in the field of environmental science and engineering.

For the past decades, zero-valent iron has been used for groundwater and wastewater remediation (Zhang et al., 2011; Choi et al., 2012). And many studies showed that zero-valent iron had a capacity to remove refractory organic pollutants

(Loraine et al., 2001; Dorathi et al., 2012). However, surface passivation seriously decreases the activity and capacity of zero-valent iron in terms of removing pollutants (Liang et al., 2000; Parbs et al., 2007; Cariato et al., 2012). Due to the high specific surface area and high surface reactivity, nanoscale zero-valent iron particles were paid extensive attention (Wang et al., 1997; Cheng et al., 2007). In these years, the study mainly focuses on the reduction mechanism of iron nanoparticles. And Fe_3O_4 nanoparticles, which were the main corrosion products of nanosized zero-valent iron particles, were received little attention.

Generally, Fe_3O_4 is supposed to be inert, and used as a magnetic carrier for catalysts or enzyme. Later, it's reported that Fe_3O_4 nanoparticles was of intrinsic peroxidase-like activity, and the combination with catalysts was not necessary (Gao et al., 2007). In our previous work, it's found that Fe_3O_4 was the main product of iron nanoparticles when reacting with pentachlorophenol (Cheng et al., 2010). In addition, the removal efficiency of 4-chlorophenol (4-CP) was improved when iron nanoparticles were used for a period of time (Cheng et al., 2007). It indicated that some product in the system contributed to the removal of 4-CP. In this paper, the role of nanosized Fe_3O_4, which is a product of nanosized iron, was studied. 4-CP was used as the model compound to test the catalytic activity of synthesized Fe_3O_4 nanoparticles and analysis the mechanisms for 4-CP removal. The results would provide important complement for the current reduction dechloridation mechanism of zero-valent iron nanoparticles, and be helpful for the application of nanosized iron particles.

2. Materials and methods

2.1 Chemicals and materials

4-chlorophenol (4-CP, ≥99%, reagent) was provided by Tianjin Jinke Fine Chemical Industry Research Institute. Ferric sulfate ($Fe_2(SO_4)_3$, 99%, reagent) was purchased from Nankai Fine Chemical Factory. Ferrous sulfate ($FeSO_4 \cdot 7H_2O$, 99.0%-101.0%) was supplied by Shenyang Reagent Factory. Methanol (99%, reagent), ethanol (99.7%, reagent), hydrogen peroxide (30%, reagent), sulfuric acid (98%, reagent) and Sodium hydroxide came from Beijing Chemical Factory. Argon gas (Ar, 99.99%) was supplied by Beijing Aolin Gas Company. All chemicals were of reagent grade and used without further purification.

2.2 Preparation of nanoparticles

Fe_3O_4 nanoparticles were synthesized by Massart hydrolysis method (Massart, 1981). Briefly, 100 mL mixed solution of 0.07 mol/L $Fe_2(SO_4)_3$ and 0.07 mol/L $FeSO_4$ was added dropwise to a four-necked flask containing 100 mL 1 mol/L NaOH aqueous solution at 80 ℃. The process was performed in Ar atmosphere. Fe_3O_4 nanoparticles were produced via following reaction:

$$Fe^{2+} + 2Fe^{3+} + 8OH^- \rightarrow Fe_3O_4 + 4H_2O \quad (1)$$

Synthesized Fe_3O_4 nanoparticles were deposited in Ar atmosphere, and then washed three times with deionized water, and dried in a vacuum dryer.

The morphology of synthesized Fe_3O_4 nanoparticles were observed with scanning electron microscope (SEM, Hitachi S-4500) and transmission electron microscope (TEM, Hitachi H-7650B). The crystal structure of the as-prepared nanoparticles and transformation products were characterized by X-ray powder diffraction (XRD, D8-advance) using a Rigaku D/max-RB X-ray diffractometer with Cu Kα radiation (λ=0.1542 nm). The magnetic properties were determined with vibrating sample magnetometer (VSM, 730T).

Besides, microscopic confocal Raman spectrometer (RM2000, Renishaw) was used to investigate the transformation of nanoparticles and verify the interaction between nanoparticles and 4-CP.

2.3 Experimental procedure

Batch experiments were conducted in 50 mL flask containing 15 mL solution, in which 4-CP, H_2O_2 and synthesized Fe_3O_4 nanoparticles were added with initial concentrations of 20 mg·L^{-1}, 1.0‰ and 2 g·L^{-1} , respectively. The flasks were sealed with sealing films and placed on a rotary shaker (TZ-2EH, Beijing Wode Company). The rotate speed and the temperature of reaction were set to be 150 rpm and 30 ℃, separately. Samples were withdrawn from various test groups at predetermined time intervals and then were filtrated with 0.22 μm filter film.

In the adsorption test, Fe_3O_4 nanoparticles (100 mg) were loaded into a 250-mL conical flask with cover containing 100 mL of an aqueous solution of 4-CP. The initial concentration of 4-CP was 20 mg•L^{-1}.The conical flask was placed on the same rotary shaker as above. In the reciprocating experiment, the 4-CP solutions were picked up for detecting and new 4-CP solutions were added into the flask and so on. And the particles were in the flask all the time. The initial concentration of 4-CP in each new solution was 20 mg•L^{-1} and the volume of the solution was 100 mL, too.

2.4 Analysis

4-CP and byproducts were quantified with an Agilent 1100 HPLC (Shanghai Agilent Ltd) equipped with a C^{18} column and an L-4000 UV-vis detector. The mobile phase for 4-CP consisted of 60% methanol and 40% water distilled three times. The flow rate was 1 mL/min and the detector wavelength was 280 nm for 4 –CP. Chlorine

ion was quantified with a DX-100 ion chromatogram (IC, DIONEX Company, Germany). The operational conditions were: eluent at 3.5 mM Na_2CO_3/1.0 mM $NaHCO_3$; eluent flow at 1.2 mL/min, sample loop volume at 250 μL, and run time at 6 min. Deionized water was used as blank.

3. Results and discussion

3.1 Characterization of Fe_3O_4 nanoparticles

The morphology of Fe_3O_4 nanoparticles synthesized was shown in Fig. 1. As seen in the SEM image, the samples were circular particles and relatively uniform. Most particles had a diameter of about 30 nm (the statistic data was shown in Fig A1 in Supplementary Materials). As seen in TEM image, the fine structure of the sample was fairly uniform.

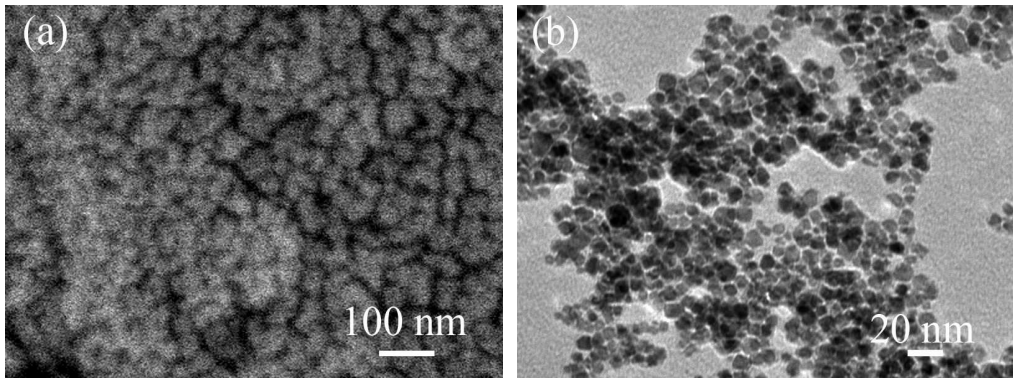

Fig. 1. The morphology of synthesized Fe_3O_4 nanoparticles: (a) SEM image; (b) TEM image.

As shown in the XRD pattern (Fig. 2), the peak position and relative intensity of as-prepared particles was consistent with that of A.R. Fe_3O_4 particles. All of the diffraction peaks can be assigned to the planes of (220), (311), (400), (422), (511) and (440) of a Fe_3O_4 structure, and the three lines were (311), (440) and (511) (JCPDS no.

26-1136). The diffraction peaks become broadened as the particle size decreases, from pattern a for A.R. Fe_3O_4 particles to pattern b for synthesized sample. No other peaks were detected in the XRD pattern, indicating the high purity of the sample.

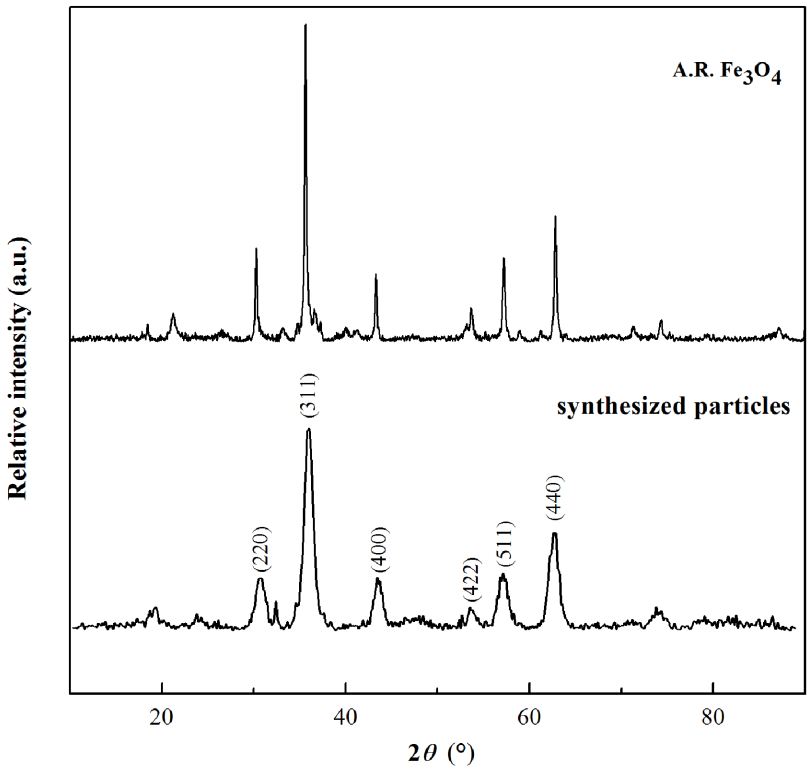

Fig. 2. XRD pattern of A.R. Fe_3O_4 particles and synthesized nanoparticles.

The magnetic property of as-prepared particles was also tested. As seen in the magnetization curve (Fig. A2 in Supplementary Materials), the saturation magnetization was 50 emu/g, and the remanence and coercivity was zero. It indicated that the synthesized particles are superparamagnetic. It meant that the synthesized particles could be reused by an external magnetic field. Actually, the particles were separated from the solution with a magnet in our experiments.

3.2 Adsorption performance of Fe_3O_4 nanoparticles

The adsorption test showed that 4-CP removed through adsorption process was

149 rather limited (Fig. 3). And no more than 10% of 4-CP was removed from solution by
150 synthesized nanoscale Fe_3O_4 particles. It is generally acknowledged that the specific
151 surface area will increase with the decrease of the particle size. And the adsorption of
152 heavy metals by nanoscale Fe_3O_4 particles had received great attention (Shen et al.
153 2009). This test showed a different result, which could due to the different surface
154 properties of the particles. As known, 4-CP is an electron acceptor. There is an extra
155 electron in Fe_3O_4, but Fe_3O_4 is not a good electron donor. As a result, the direct
156 electron transfer is not so easily between 4-CP and Fe_3O_4 (Gopalakrishnan et al. 2011).
157 In the other hand, Fe_3O_4 is magnetic and 4-CP is dipole like, there would be some
158 magnetic attraction between Fe_3O_4 and 4-CP. However, the removal efficiency of
159 4-CP did not figure it out.

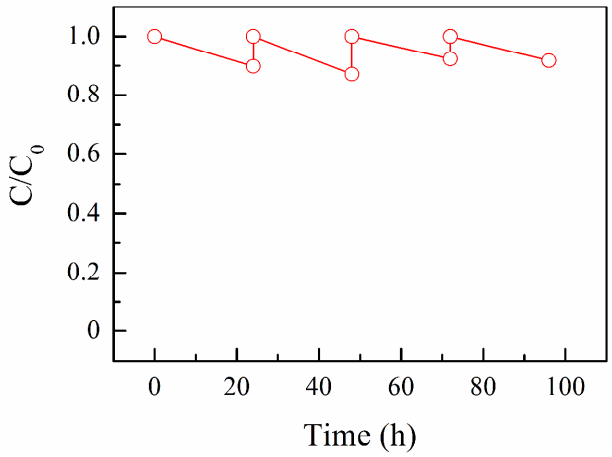

160

161 Fig. 3. Adsorption of 4-CP with synthesized Fe_3O_4 nanoparticles.

162 To understand the surface property of as-prepared Fe_3O_4 nanoparticles and the
163 interaction between 4-CP and Fe_3O_4, the Raman spectrum of Fe_3O_4 nanoparticles
164 before and after adsorption was determined. As shown in Fig. 4, there was a strong
165 peak at 665 cm^{-1} in both of the samples, which was the characteristic peak of Fe_3O_4
166 (Xue et al., 2009). And in the spectrum of the sample after reaction, there were other

two weak peaks at 380 cm^{-1} and 295 cm^{-1}, respectively. It might be produced by molecular vibration of 4-CP adsorbed on the surface of Fe_3O_4 particles. The signal from Raman spectrum indicated that there was some interaction between 4-CP and Fe_3O_4 particles, although the action was really weak. It's speculated that the physical adsorption was occurred between 4-CP and Fe_3O_4 particles, and the low amount of adsorption led to the weak peak (Lin et al. 2015).

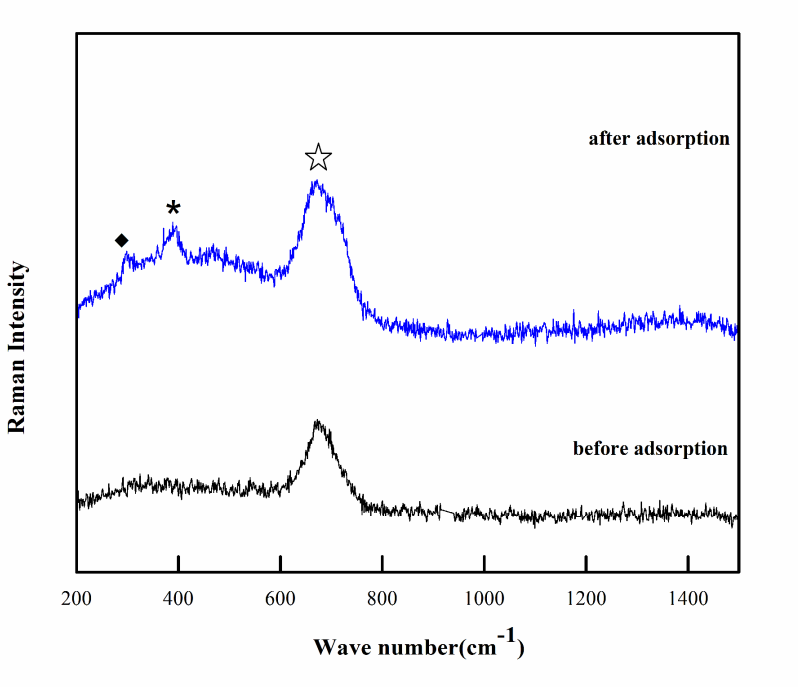

Fig. 4. Raman spectrum of Fe_3O_4 nanoparticles before and after adsorption.

3.3 Removal of 4-CP

It is well known that pH value has a significant effect on the formation of hydroxyl radicals (·OH) and the removal of pollutants in Fenton/Fenton-like systems. The removal of 4-CP with synthesized Fe_3O_4 nanoparticles at different pH values were tested in this study. As shown in Fig. 5, the compound was completely removed within 4 h in acid condition. On the contrary, the removal rate at pH=7.0 or 8.0 was about 40% even though the reaction extended to 30 h. Therefore, the degradation rate

of 4-CP at low pH value was absolutely higher than that at high pH value. It was similar to the Fenton systems (Zhou et al., 2008; Li et al., 2015). Different from the conventional Fenton system, the organic pollutant could still be degraded to a certain extent in neutral and alkaline conditions. At low pH value, the results can be attributed to: (1) the high oxidation capacity of hydroxyl radicals (·OH), which was responsible for the removal and oxidation of chlorophenol; (2) more hydroxyl radicals (·OH) were generated via Fenton reaction (Kim et al., 2010); (3) less adsorption of iron hydroxides on the surface of particles (Masomboon et al., 2009); (4) relatively stability of H_2O_2 (Zhang et al., 2009).

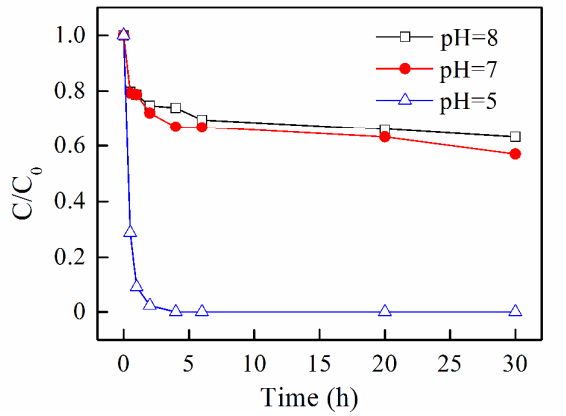

Fig. 5. Removal of 4-CP at different pH values

Based on previous studies, the removal mechanism was involved in dechlorination in the system (Xu et al., 2009; Jia et al., 2012; Xu et al., 2013). So the chlorine ion in the system was determined. And a similar phenomenon was attained from the perspective of chlorine ion release. A significant higher dechlorination rate was obtained in acid condition compared to neutral and alkaline conditions (Fig. 6). And the dechlorination rate showed a trend of growth in acid condition. Especially, when 4-CP was completely removed after reacting for 4 h, the dechlorination rate was just 48.8%, and later dechlorination continued. When the time extended to 30 h, the

dechlorination rate was 83.9%.

Comparing the dechlorination rate of 4-CP (Fig. 6) with the removal rate (Fig. 5) at different pH values, apparently, the dechlorination rate was lower than the removal rate in each system, which suggested that there were other processes involved in the removal of 4-CP in addition to dechlorination. On the one hand, it could be physical processes such as adsorption, volatilization, etc; on the other hand, chlorine compounds may be produced. As determined in section 3.2, the physical adsorption contributed little to the removal of 4-CP. Besides, the volatilization of 4-CP is so weak that the volatilization process could be neglected. Therefore, the suspect was likely to be chlorine compounds, which will be elaborated in section 3.6.

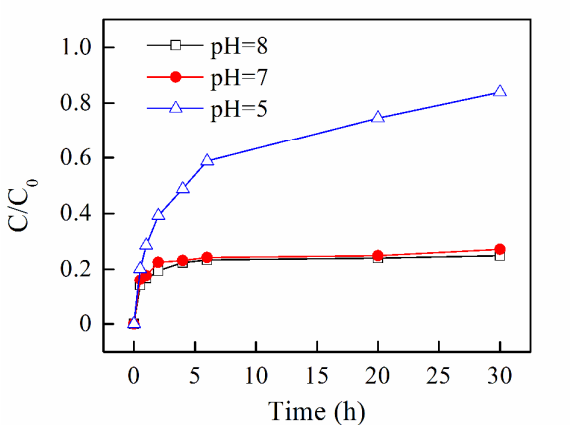

Fig. 6. Dechlorination of 4-CP at different pH values.

3.4 Removal of 4-CP by reused Fe_3O_4 nanoparticles

In order to study whether the residual particles had the catalysis ability to remove 4-CP, a series of tests were carried out at different pH values. As shown in Fig 7(a), 4-CP can be completely removed in 0.5 h with the reused Fe_3O_4 particles in repeated experiments. It indicated that synthesized Fe_3O_4 nanoparticles still had an excellent catalysis activity even after being used for a few times. When the initial pH value was 8, the removal rate was obviously lower (Fig. 7(b)). However, the results showed

similar trend when Fe_3O_4 particles were reused. The removal of 4-CP was enhanced when Fe_3O_4 nanoparticles were reused in the systems. It was speculated that the reaction sites were changed on the surface of Fe_3O_4 nanoparticles, which improved the oxidation of 4-CP. Besides, long time reaction made a significant contribution to the morphological change of Fe_3O_4 nanoparticles (details were demonstrated in section 3.5).

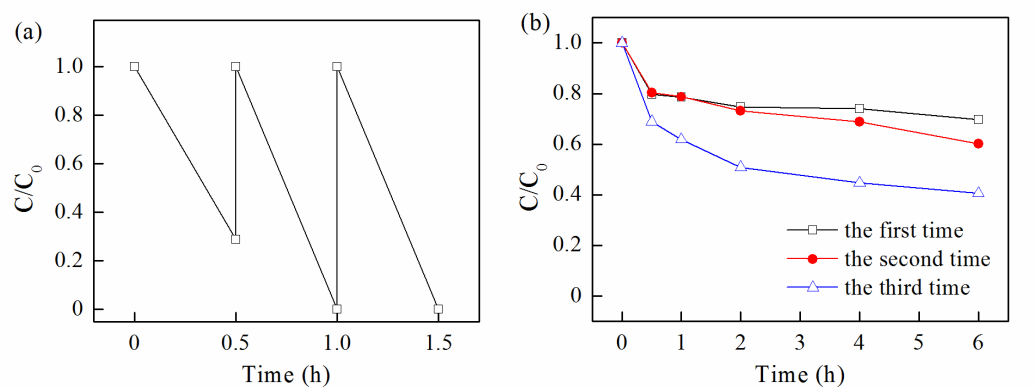

Fig .7. Removal of 4-CP with reused Fe_3O_4 nanoparticles: (a) initial pH=5.0; (b) initial pH=8.0.

3.5 The transformation of Fe_3O_4 nanoparticles

The morphology of Fe_3O_4 nanoparticles presented little change after reaction without hydrogen peroxide and were still evenly dispersed small particles (Fig A3 in Supplementary Materials). However, things were totally different when hydrogen peroxide was added into the system. Although Fe_3O_4 remained as scattered small particles in a short period, the nanoparticles would develop into chain, flower structure as reaction proceed, namely formed rough surface. As shown in Fig. 8, particles were eroded, aggregated, finally larger flakes were generated. The existence of erosion points were the sources of surface active sites of Fe_3O_4 particles. And in the other studies, some surface defects of nanoscale iron were also formed, which could

be used as active sites in the process of dechlorination (Gotpagar et al., 1999; Zhou et al., 2008).

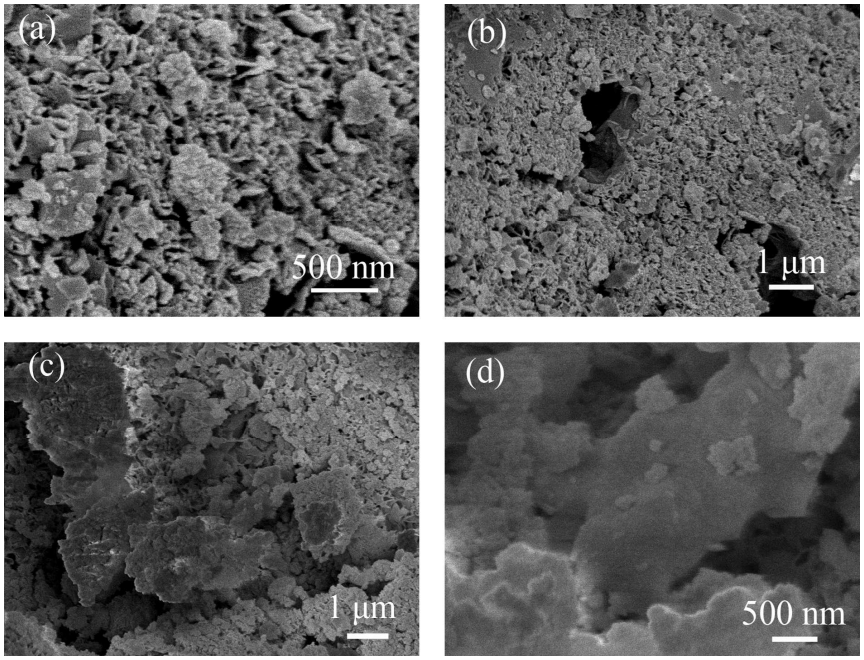

Fig. 8. SEM images of Fe_3O_4 nanoparticles after reaction with H_2O_2 present. (a)~(c) showed the particles after reacting for different periods. (d) was the amplification of image (c).

The XRD pattern revealed that the composition of Fe_3O_4 nanoparticles had little change before and after reaction (Fig 9). And the result further confirmed that Fe_3O_4 nanoparticles acted as a catalyst in the system. There was no impurity peak detected, indicating there was no new solid matter produced, and no phrase change in the reaction process occurred to nanoparticles.

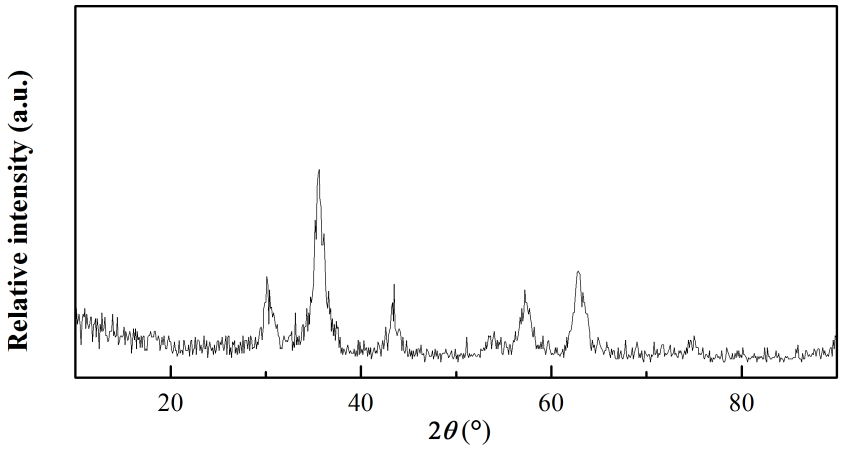

Fig. 9. XRD pattern of Fe_3O_4 after reacting with 4-CP (with H_2O_2 present).

To investigate the changes of surface properties of particles, Raman spectrum of Fe_3O_4 nanoparticles before and after reaction was determined. Similarly to Fig 4, strong peaks (Fe_3O_4) were detected in all samples at 665 cm^{-1} (Fig. 10). Besides, weak peaks at 358 cm^{-1} and 488 cm^{-1} were detected in the sample after being used once, which might be brought by 4-CP and its products. However, the peaks were not detected in the sample after being used twice. It revealed that there were certain interactions, but very weak physical adsorption happened between the surface of nanoparticles and chlorophenol. And there were no peaks detected yet in the sample after reacting for 30 h without H_2O_2 except the 665 cm^{-1} one, which was different with the previous result (Fig. 4). It meant that the peaks disappeared brought by 4-CP adsorbed on the surface of Fe_3O_4 particles after a long time reaction. The result confirmed that it's a physical adsorption between 4-CP and Fe_3O_4 particles, and desorption could easily occur. That's a dynamic process, so the weak peaks could just be detected sometimes.

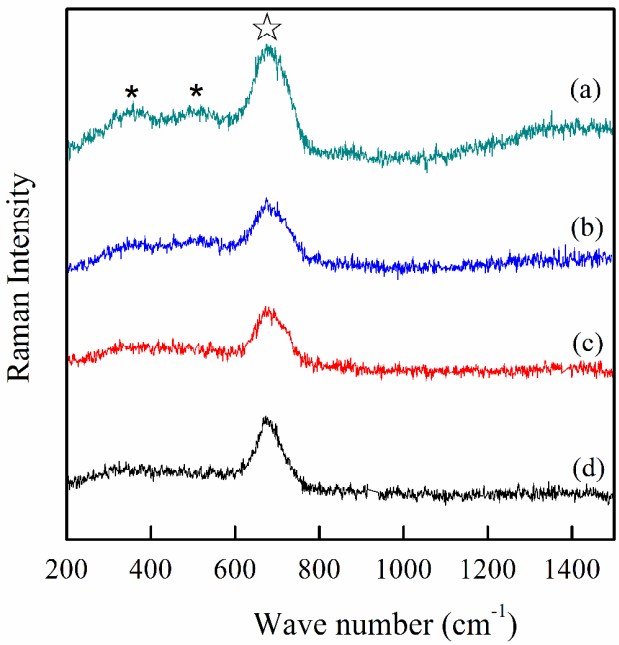

Fig. 10. Raman spectrum of Fe_3O_4 nanoparticles before and after reaction: (a) after being used once; (b) after being used twice; (c) without H_2O_2; (d) before reaction.

3.6 The mechanism of 4-CP removal

Based on the above analysis, the catalytic oxidation of 4-CP by Fe_3O_4 nanoparticles was a surface reaction process. The Fenton-like reaction between Fe_3O_4 nanoparticles and hydrogen peroxide occurred as following:

$$Fe^{2+} + H_2O_2 + H^+ \rightarrow Fe^{3+} + H_2O + \cdot OH \quad (2)$$

$$Fe^{2+} + \cdot OH \rightarrow Fe^{3+} + OH^- \quad (3)$$

$$H_2O_2 + \cdot OH \rightarrow H_2O + \cdot O_2H \quad (4)$$

$$Fe^{3+} + H_2O_2 \rightarrow Fe^{2+} + H^+ + \cdot O_2H \quad (5)$$

$$\cdot O_2H \mid Fe^{3+} \rangle Fe^{2+} \mid \cdot O_2 \mid H^+ \quad (6)$$

$$\cdot O_2H \rightarrow \cdot H + \cdot O_2 \quad (7)$$

$$\cdot OH + 4\text{-}CP \rightarrow Cl^- + intermediates \quad (8)$$

$$\cdot OH + 4\text{-}CP \rightarrow Cl\text{-}R \quad (9)$$

The reaction (1) played a significant role in the 4-CP removal due to the generation of hydroxyl radical. And it also explained that acid condition was conducive to chain reactions and greatly improved the oxidation rate of 4-CP.

In the section 3.3, chlorine ion was detected. It well explained (in Eq. 8) that the chlorine atom of 4-CP was attacked by hydroxyl radical, which led to the chlorine atom located in the para-position of 4-CP was substituted (Li et al., 1999; Zhou et al., 2008; Huang et al., 2015). As a result, the chlorine ions were released into solution. Besides, the dechlorination rate was absolutely lower than the removal rate, which suggested that chlorine compounds were generated through different reaction pathways (Zhou et al., 2008; Huang et al., 2015). And the byproducts in the solution might affect the dechlorination of 4-CP by Fe_3O_4 nanoparticles (Xu et al., 2013). Fig. 11 demonstrated the mechanism of catalytic oxidation of 4-CP by Fe_3O_4 nanoparticles.

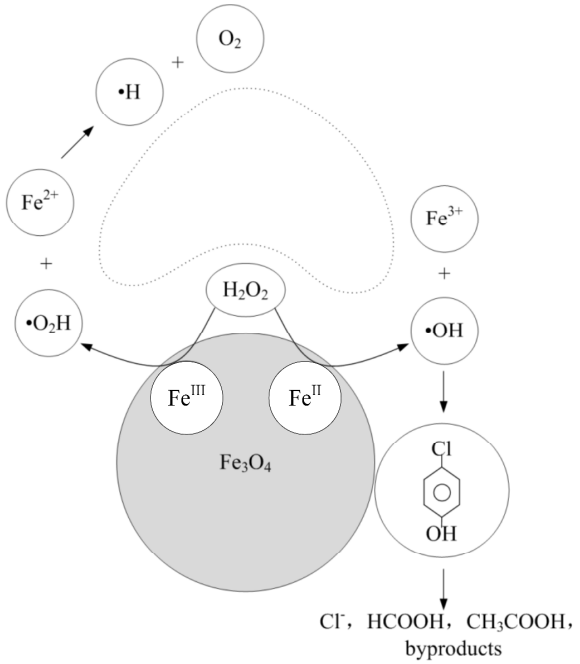

Fig. 11. The mechanism sketch of catalytic oxidation of 4-CP by Fe_3O_4 nanoparticles.

296 Moreover, there was an obvious decline of pH value in each solution system over
297 time in above studies (Fig. A4 in Supplementary Materials), which indicated amount
298 of acidic matter was generated during reaction, in accordance with published study
299 (Zhou et al., 2008). In fact, formic acid and acetic acid were detected in the system,
300 which indicated that the carbon-carbon double bond of benzene ring was broken down
301 and then made the formation of acid matter be possible during the reaction (Zazo et al.,
302 2005; Zhou et al., 2008).
303 In addition, intermediates were also detected from HPLC spectrum (Fig. A5 in
304 Supplementary Materials).

305 **4. Conclusions**

306 (1) The removal rate and dechlorination rate of 4-CP in acid condition was absolutely
307 higher than that in neutral and alkline conditions. However, 4-CP could also be
308 degraded under neutral and alkali conditions.
309 (2) Synthesized Fe_3O_4 nanoparticles showed high catalytic activity even after being
310 used several times. Especially, the activity was improved after being used.
311 (3) The surface morphology of Fe_3O_4 nanoparticles changed a lot and the reactive
312 sites on the surface increased which resulted in the higher activity of particles
313 after being used.
314 (4) Adsorption process didn't play an important role for 4-CP removal, but it did
315 occur between 4-CP and Fe_3O_4. Hydroxyl radical produced through Fenton
316 reaction made an outstanding contribution to the degradation of 4-CP.

317

Acknowledgement

This work was supported by the Fundamental Research Funds for the Central Universities, and the Research Funds of Renmin University of China (Grant No. 11XNK016), which are greatly acknowledged.

References

Cariato, L., Schoup, G., Seuntjens, P., 2012. Predicting longevity of iron permeable reactive barriers using multiple iron deactivation models. J. Contam. Hydrol. 142, 93-108.

Cheng, R., Wang, J. L., Zhang, W. X., 2007. Comparison of reductive dechlorination of p-chlorophenol using Fe^0 and nanosized Fe^0. J. Hazard. Mater. 144 (1-2), 334-339.

Cheng, R., Zhou, W, Wang, J. L., Qi, D. D., Guo, L., Zhang W. X., Qian, Y., 2010. Dechlorination. of pentachlorophenol using nanoscale Fe/Ni particles: role of nano-Ni and its size effect. J. Hazard. Mater. 180(1-3), 79-85.

Choi, K., Lee, W., 2012. Enhanced degradation of trichloroethylene in nano-scale zero-valent iron Fenton system with Cu (II). J. Hazard. Mater. 211-212, 146-153.

Dorathi, P. J., Kandasany, P., 2012. Dechlorination of chlorophenols by zero valent iron impregnated silica. J. Environ. Sci. 24 (4), 765-773.

Gao, L. Z., Zhuang, J., Nie, L., 2007. Intrinsic peroxidase-like activity of ferromagnetic nanoparticles. Nat. Nanotechnol. 2(9), 577-583.

Gotpagar, J., Lyuksyutov, S., Cohn, R., Grulke, E., Bhattacharyya, D., 1999. Reductive dehalogenation of trichloroethylene with zero-valent iron: Surface profiling microscopy and rate enhancement studies. Langmuir. 15, 8412-8420.

Gopalakrishnan, K., Joshi, H. M., Kumar, P., Panchakarla, L. S., Rao, C. N. R., 2011.

342 Selectivity in the photocatalytic properties of the composites of TiO_2 nanoparticles
343 with B-and N-doped graphenes. Chem. Phys. Lett. 511, 304-308.
344 Huang, Q., Cao, M. H., Ai, Z. H., Zhang, L. Z., 2015. Reactive oxygen species
345 dependent degradation pathway of 4-chlorophenol with $Fe@Fe_2O_3$ core-shell
346 nanowires. Appl. Catal. B: Environ. 162, 319-326.
347 Hwang, Y., Mines, P. D., Jakobsen, M. H., Andersen, H. R., 2015. Simple
348 colorimetric assay for dehalogenation reactivity of nanoscale zero-valent iron using
349 4- chlorophenol. Appl. Catal. B: Environ. 166-167, 18-24.
350 Jia, H. Z., Wang, C.Y., 2012. Adsorption and dechlorination of 2,4-dichlorophenol
351 (2,4-DCP) on a multi-functional organo-smectite templated zero-valent iron
352 composite. Chem. Eng. J. 191, 202-209.
353 Kim, J. Y., Lee, C. H., Sedlak, D. L., Yoon, J., Nelson, K. L., 2010. Inactivation of
354 MS2 coliphage by Fenton's reagent. Water. Res. 44, 2647-2653.
355 Li, R. C., Jin, X. Y., Megharaj, M., Naidu, R., Chen, Z. L., 2015. Heterogeneous
356 Fenton oxidation of 2,4-dichlorophenol using iron-based nanoparticles and
357 persulfate system. Chem. Eng. J. 264, 587-594.
358 Li, X. J., Cubbage, J.W., Tetzlaff, T. A., Jenks, W. S., 1999. Photocatalytic
359 degradation of 4-chlorophenol. 1. The hydroquinone pathway. J. Org. Chem. 64,
360 8509-8524.
361 Liang, L.Y., Korte, N., Gu, B.H., 2000. Geochemical and microbial reactions
362 affecting the long-term performance of in situ "iron barriers". Adv. Environ. Res.
363 4(4): 273-286.
364 Lin, D., Kumar, P., Jin, S., Liu, S., Nian, Q., Cheng, G. J., 2015. Laser direct writing
365 of crystalline Fe_2O_3 atomic sheets on steel surface in aqueous medium. Appl. Surf.
366 Sci. 351, 148-154.

Loraine, G. A., 2001. Effects of alcohols, anionic and nonionic surfactants on the reduction of TEC by zero-valent iron. Water. Res. 35 (6), 1453-1460.

Masomboon, N., Ratantamskul, C., Lu, M. C., 2009. Chemical oxidation of 2,6-Dimethylaniline in the Fenton Process. Environ. Sci. Technol. 43 (22), 8629-8634.

Massart, R., 1981. Preparation of aqueous magnetic liquids in alka–line and acidic media. IEEE Trans Magnetics, 17, 1247.

Parbs, A., Ebert, M., Dahmke, A., 2007. Long-term effects of dissolved carbonate species on the degradation of trichloroethylene by zerovalent iron. Environ. Sci. Technol. 41(1), 291-296.

Ruzgas, T., Emneus, J., Gorton, L., Marko, V. G., 1995. The development of a peroxidase biosensor for monitoring phenol and related aromatic compounds. Anal. Chem. Acta. 31(3), 245-253.

Shen, Y. F., Tang, J., Nie, Z. H., et al. 2009. Tailoring size and structural distortion of Fe_3O_4 nanoparticles for the purification of contaminated water. Bioresource. Technol. 100(18): 4139-4146.

Wang, C. B., Zhang, W. X., 1997. Synthesizing nanoscale iron particles for rapid and complete dechlorination of TCE and PCBs. Environ. Sci. Technol, 31(7): 2154-2156.

Xu, J., Tan, L. S., Baig, S. A., Wu, D. L., Lv, X. S., Xu, X. H., 2013. Dechlorination of 2,4-dichlorophenol by nanoscale magnetic Pd/Fe particles: Effect of pH, temperature, common dissolved ions and humic acid. Chem. Eng. J. 231, 26-35.

Xu, J. X., Tang, J., Baig, S. A., Lv, X. S., Xu, X. H., 2013. Enhanced dechlorination of 2,4-dechlorophenol by Pd/Fe-Fe_3O_4 nanocomposites. J. Hazard. Mater. 244-245,

628-636.

Xu, X. H., Wo, J. J., Zhang, J. H., Wu, Y. J., Liu, Y., 2009. Catalytic dechlorination of p-NCB in water by nanoscale Ni/Fe. Desalination. 242 (1-3), 346-354.

Xue, X., Hanna, K., Abdelmoula, M., 2009. Adsorption and oxidation of PCP on the surface of magnetite: Kinetic experiments and spectroscopic investigations. Appl. Catal. B Environ. 89, 432-440.

Zazo, J. A., Casas, J. A., Mohedano, A. F., Gilarranz, M. A., Rodreguez, J. J., 2005. Chemical pathway and kinetics of phenol oxidation by Fenton's reagent. Environ. Sci. Technol. 39 (23), 9295–9302.

Zhang, X., Lin, S., Chen, Z.L., Megharaj, M., Naidu, R., 2011. Kaolinite-supported nanoscale zero-valent iron for removal of Pb from aqueous solution: reactivity, characterization and mechanism. Water. Res. 3481-3488.

Zhang, W. H., Quan, X., Zhang, Z. Y., 2007. Catalytic reductive dechlorination of p-chlorophenol in water using Ni/Fe nanoscale particles. J. Environ. Sci. 19 (3), 362-366.

Zhang, S. X., Zhao, X. L., Niu, H. Y., Shi, Y. L., Cai, Y. Q., Jiang, G. B., 2009. Superparamagnetic Fe_3O_4 nanoparticles as catalysts for the catalytic oxidation of phenolic and aniline compounds. J. Hazard. Mater. 167 (1-3), 560-566.

Zhou, T., Li, Y. Z., Ji, J., Wong, F. S., Lu, X. H., 2008. Oxidation of 4-chlorophenol in a heterogeneous zero valent iron/H_2O_2 Fenton-like system: Kinetic, pathway and effect factors. Sep. Purif. Technol. 62 (3), 551-558.